

# Supramolecular and Intramolecular Energy Transfer with Ruthenium–Anthracene Donor–Acceptor Couples: Salt Bridge versus Covalent Bond

Jonathan C. Freys<sup>[a]</sup> and Oliver S. Wenger<sup>\*[a]</sup>

**Keywords:** Energy transfer / Donor–acceptor systems / Supramolecular chemistry / Ruthenium / Hydrogen bonds

The formation of hydrogen-bonded cation–anion adducts between the complex  $[\text{Ru}(\text{bpy})_2(\text{biimH}_2)]^{2+}$  (bpy = 2,2'-bipyridine; biimH<sub>2</sub> = 2,2'-biimidazole) and anthracene-9-carboxylate in dichloromethane solution was investigated by <sup>1</sup>H NMR, optical absorption, and luminescence spectroscopy. The experimental data indicates that more than one anthracene-9-carboxylate anion can interact closely with the dicat-

ionic ruthenium complex. Energy transfer from the photoexcited ruthenium complex to anthracene-9-carboxylate in 1:1 adducts of these two components was investigated by transient absorption spectroscopy and compared to intramolecular energy transfer in a covalently linked ruthenium-xylylene-anthracene dyad with a comparable donor–acceptor distance.

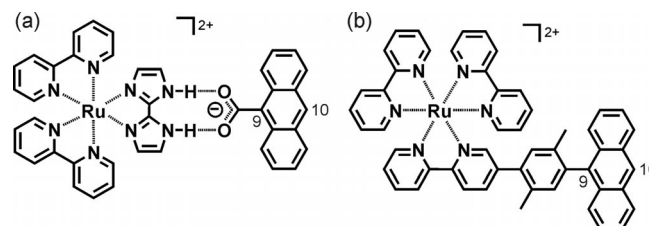
## Introduction

Cation–anion interactions play an important role in the vast field of ion sensing,<sup>[1]</sup> and hydrogen-bonded cation–anion pairs are key structural elements in many supramolecular assemblies.<sup>[2]</sup> In proteins, salt bridges between arginine and aspartate or glutamate are crucial to stabilizing the tertiary structure.<sup>[3]</sup> The extent to which hydrogen bonds can mediate charge and energy transfer is of significant biological relevance, and in this context there have been numerous investigations of hydrogen-bond-mediated electron transfer.<sup>[4,5]</sup> This includes, for example, hydrogen-bonded cation–anion adducts between amidinium cations and carboxylates that mimic the naturally occurring salt bridges mentioned above.<sup>[6]</sup> Cationic metal complexes of 2,2'-biimidazole (biimH<sub>2</sub>) and 2,2'-bibenzimidazole (bibzimH<sub>2</sub>) have been reported to form hydrogen-bonded pairs with carboxylates<sup>[7]</sup> as well as other anions,<sup>[8]</sup> and this has opened the possibility for investigations of photoinduced charge<sup>[9]</sup> and energy transfer<sup>[10]</sup> within such adducts.

The basic optical spectroscopic and electrochemical properties of many ruthenium and osmium complexes with biimH<sub>2</sub> and bibzimH<sub>2</sub> have been explored more than twenty years ago.<sup>[11]</sup> Several complexes with related ligands have been reported in the meantime.<sup>[12]</sup> In recent years, photoredox-active complexes with ligands that can be deprotonated, including biimH<sub>2</sub>, bibzimH<sub>2</sub>, and related pyridyl imid-

azoles, experience a revival that appears to be mostly driven by the increasing interest in proton-coupled electron-transfer reactions.<sup>[9,13]</sup>

In this paper, we report on the interaction of the dicationic complex  $[\text{Ru}(\text{bpy})_2(\text{biimH}_2)]^{2+}$  (bpy = 2,2'-bipyridine) with anthracene-9-carboxylate anions in dichloromethane solution. Experimental evidence suggests that, in solutions containing equimolar quantities of these two components, hydrogen-bonded cation–anion adducts (Scheme 1a) that have large association constants form, as observed previously for other biimidazole complexes and carboxylate anions.<sup>[7–8]</sup> When excess anthracene-9-carboxylate is used, abrupt changes in the <sup>1</sup>H NMR spectra indicate that more than one of these particular monoanions may interact closely with the  $[\text{Ru}(\text{bpy})_2(\text{biimH}_2)]^{2+}$  dication. Photoinduced energy transfer from the ruthenium complex to the anthracene core in the 1:1 salt bridge adduct in Scheme 1a was explored by transient absorption spectroscopy and compared to energy transfer in the covalent donor-bridge-acceptor molecule in Scheme 1b. This comparison provides



Scheme 1. (a) Molecular structure of a hydrogen-bonded 1:1 adduct between the dicationic complex  $[\text{Ru}(\text{bpy})_2(\text{biimH}_2)]^{2+}$  (bpy = 2,2'-bipyridine; biimH<sub>2</sub> = 2,2'-biimidazole) and an anthracene-9-carboxylate monoanion; (b) formula of the covalent donor-bridge-acceptor molecule synthesized and investigated in this work.

[a] Institut für Anorganische Chemie, Georg-August-Universität Göttingen, Tammannstraße 4, 37077 Göttingen, Germany  
Fax: +49-551-39-3373  
E-mail: oliver.wenger@chemie.uni-goettingen.de

Supporting information for this article is available on the WWW under <http://dx.doi.org/10.1002/ejic.201000815>.

insight into the relative magnitudes of the electronic donor–acceptor couplings that are mediated by salt bridges and covalent linkers.

## Results and Discussion

Figure 1 shows the results of a  $^1\text{H}$  NMR spectroscopic titration of  $[\text{Ru}(\text{bpy})_2(\text{biimH}_2)]^{2+}$  with anthracene-9-carboxylate in deuteriated dichloromethane. In all spectra, the resonances due to protons attached to carbon atoms of the biimidazole ligand are observable as two singlets (marked by two squares in Figure 1) at chemical shifts below 7.30 ppm, well-separated from all other signals. Resonances due to nitrogen-bound protons remain unobserved even in carefully dried deuteriated solvents.

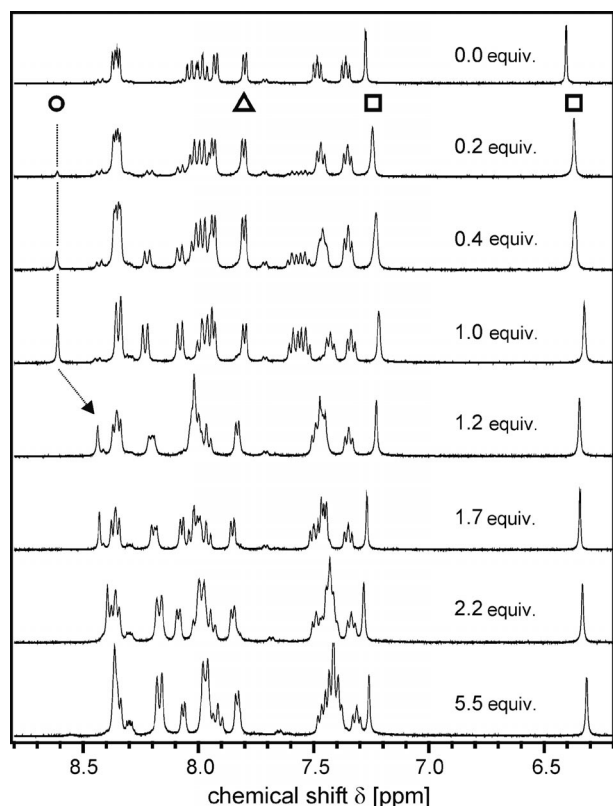


Figure 1.  $^1\text{H}$  NMR spectra of a 1.15 M solution of  $[\text{Ru}(\text{bpy})_2(\text{biimH}_2)]^{2+}$  in  $\text{CD}_2\text{Cl}_2$  in the presence of varying amounts of anthracene-9-carboxylate.

In the spectrum of the ruthenium complex alone (uppermost spectrum), the two biimidazole proton resonances are observed at  $\delta = 7.28$  and  $6.41$  ppm. Upon addition of up to 1 equiv. of anthracene-9-carboxylate, these signals experience upfield shifts of 0.06 and 0.08 ppm, respectively, while the signals due to bipyridine protons, for example the doublet at  $\delta = 7.81$  ppm (marked by a triangle in Figure 1), are virtually unaffected. Similar upfield shifts for the biimidazole resonances have been observed previously for an iridium biimidazole complex that was titrated with various benzoate anions.<sup>[9a]</sup> When one of the nitrogen atoms of the biimidazole ligand in  $[\text{Ru}(\text{bpy})_2(\text{biimH}_2)]^{2+}$  is deprotonated by tetrabutylammonium hydroxide, the four biimidazole C–

H protons still give rise to only two singlets, indicating that proton exchange between the two nitrogen atoms is fast on the NMR spectroscopic timescale (data not shown). However, the two singlets are now shifted upfield by 0.14 and 0.19 ppm, respectively. As in the prior iridium study,<sup>[9a]</sup> the upfield shifts observed in Figure 1 after addition of anthracene-9-carboxylate are therefore interpreted in terms of hydrogen-bonding interactions occurring between the cation and the carboxylate anion. In the course of hydrogen-bond formation, proton density is localized away from the biimidazole nitrogen atoms, which results in an upfield shift that is somewhat smaller than the one associated with the removal of an entire proton. Thus, for up to 1 equiv. of anthracene-9-carboxylate added, Scheme 1a is likely to give a reasonable representation of the interaction between the cationic ruthenium complex and anthracene-9-carboxylate in dichloromethane: Both biimidazole N–H protons are likely to be involved in hydrogen bonding to the two oxygen atoms of the carboxylate anion, thereby forming a salt bridge that resembles those occurring between amidinium and carboxylate groups in artificial and biological systems. Structures of several biimidazole complexes determined by single-crystal X-ray diffraction suggest that twofold hydrogen bonding with this ligand is possible thanks to significant bending of its two imidazole moieties relative to one another upon coordination to a metal center,<sup>[7a,7c,7d,8a,8b,9a]</sup> leading to N–O distances between 2.3 and 2.7 Å in the case of carboxylate binding partners.<sup>[7c,7d,9a]</sup>

When the added quantity of anthracene-9-carboxylate titrant surpasses 1 equiv., the trend in the upfield shift of the biimidazole resonances below 7.30 ppm is not continued. Already at 1.2 equiv., the two signals are shifted further downfield relative to those at 1 equiv., and this new trend continues at 1.7 and 2.2 equiv. However, much more obvious than these relatively minor shifts of the biimidazole resonances is the evolution of a signal associated with anthracene-9-carboxylate: The resonance caused by the isolated proton at the 10-position of this anion initially occurs as a singlet at  $\delta = 8.61$  ppm (marked by a circle in the spectrum at 0.2 equiv.), and it remains at the same chemical shift up to 1 equiv. (dashed vertical line). At 1.2 equiv., this signal is observed at  $\delta = 8.43$  ppm, a displacement by 0.18 ppm with respect to its initial chemical shift (arrow in Figure 1). Subsequently, this resonance is shifted further upfield.

In Figure 2, the chemical shifts of four different resonances from Figure 1 are plotted against the relative amount of anthracene-9-carboxylate added to the  $[\text{Ru}(\text{bpy})_2(\text{biimH}_2)]^{2+}$  solution. The uppermost panel (a) is for the above-mentioned proton at the 10-position of anthracene-9-carboxylate, while the two lowest panels (c, d) illustrate the evolution of the biimidazole C–H resonances. The fourth panel (b) is for an NMR signal that is due to the bipyridine ligands of the ruthenium complex.

Common to all four signals in Figure 2 is the discontinuity between 1 and 1.2 equiv. While the anthracene-9-carboxylate and bipyridine signals (a, b) occur at virtually unchanged chemical shifts between 0 and 1.0 equiv., the biimidazole signals (c, d) undergo upfield displacements due

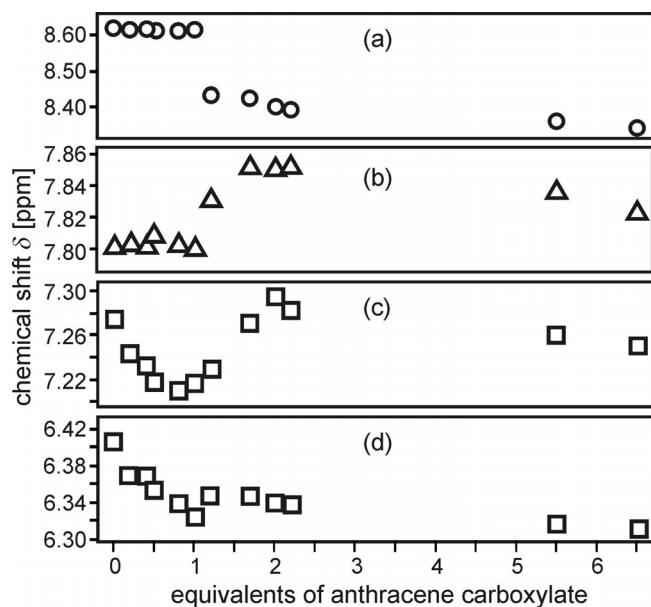


Figure 2. Chemical shifts of four characteristic  $^1\text{H}$  NMR resonances from Figure 1: (a) anthracene-9-carboxylate singlet due to the proton attached at the 10-position; (b) doublet signal due to bipyridine ligands of  $[\text{Ru}(\text{bpy})_2(\text{biimH}_2)]^{2+}$ ; (c, d) singlet signals due to carbon-bound biimidazole protons of  $[\text{Ru}(\text{bpy})_2(\text{biimH}_2)]^{2+}$ .

hydrogen-bonding interactions as discussed above. The discontinuities at 1 equiv. preclude determination of the association constant ( $K_a$ ) for the biimidazole–carboxylate interaction, but prior studies have revealed  $K_a$  values of the order of  $10^5$ – $10^6 \text{ M}^{-1}$  for this type of salt bridge.<sup>[9a,10]</sup> The fact that there is a discontinuity for all four signals in Figure 2 strongly suggests that the type of cation–anion interaction changes fundamentally when more than 1 equiv. of anthracene-9-carboxylate is present in solution, that is, Scheme 1a does not give an accurate representation of the situation under such conditions. The fact that the discontinuities occur already at 1.2 equiv. of anthracene-9-carboxylate suggests that two such anions interact rather strongly with the divalent ruthenium complex. Such behavior remained unobserved in the NMR spectroscopic titration of an iridium biimidazole complex with benzoate anions, presumably because the respective metal complex was only singly charged.<sup>[9a]</sup> The NMR spectroscopic titration data for the ruthenium(II) systems here suggest that the molecular ensemble comprising one ruthenium complex and two anthracene-9-carboxylate anions is very stable, possibly because of favorable interactions between two anthracene moieties. The displacement of the anthracene singlet from 8.61 to 8.43 ppm may be a manifestation of  $\pi$ -interactions that involve the anthracene backbone, but the simultaneous shift of the bipyridine doublet from 7.81 to 7.85 ppm (Figure 2b) may indicate that bipyridine ligands are also involved in intermolecular interactions. However, the actual structure of these molecular ensembles in solution remains unclear, and a solid-state structure is not available either. At any rate, the key point here is that there seem to be rather strong interactions between one ruthenium(II) complex and two anthracene-9-carboxylate anions.

Cation–anion interactions also manifest themselves in optical absorption spectra. Figure 3a shows the metal-to-ligand charge transfer (MLCT) absorption band of  $[\text{Ru}(\text{bpy})_2(\text{biimH}_2)]^{2+}$  in  $3 \times 10^{-5} \text{ M}$  dichloromethane solution in the presence of 0.00, 0.15, 0.31, and 1.25 equiv. of anthracene-9-carboxylate. The lowest-energy MLCT transition in this heteroleptic complex has been identified previously as a ruthenium(II)-to-biimidazole transition,<sup>[11a]</sup> while the ruthenium(II)-to-bipyridine transitions occur at somewhat higher energies. Upon addition of anthracene-9-carboxylate, the MLCT absorption band maximum redshifts from its initial position at 477 nm to 494 nm at 1.25 equiv. (Figure 3a), but continuing to add anthracene-9-carboxylate does not induce any further significant changes in the MLCT absorption band.

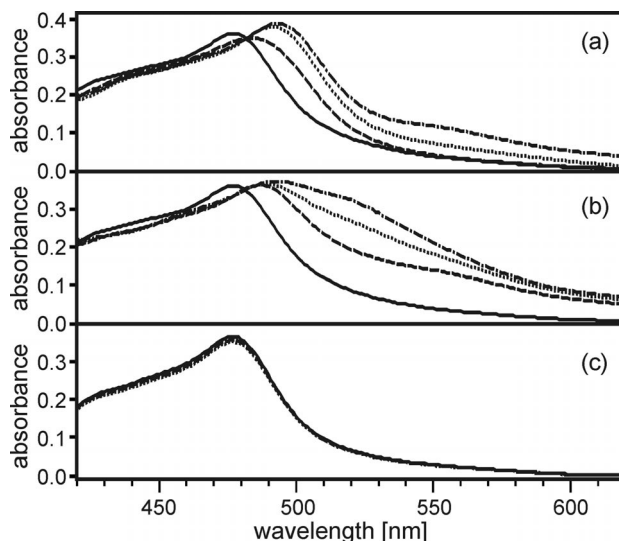


Figure 3. Metal-to-ligand charge transfer (MLCT) absorption band of  $[\text{Ru}(\text{bpy})_2(\text{biimH}_2)]^{2+}$  in  $3 \times 10^{-5} \text{ M}$   $\text{CH}_2\text{Cl}_2$  solution in the presence of various titrants: (a) anthracene-9-carboxylate; (b) tetrabutylammonium hydroxide; (c) unsubstituted anthracene. Solid lines: 0.00 equiv.; dashed lines: 0.15 equiv.; dotted lines: 0.31 equiv.; dash-dotted lines: 1.25 equiv.

As indicated in Figure 3b, deprotonation of the biimidazole nitrogen atoms leads to qualitatively similar changes in the MLCT band,<sup>[11a]</sup> and the band maximum redshifts to 495 nm at 1.25 equiv. In addition, in the case of hydroxide addition, the MLCT band broadens substantially as a result of increasing absorption intensity at longer wavelengths. Thus, as for the NMR spectroscopic data, there are strong analogies between the effects of salt bridge formation and deprotonation. Figure 3c shows that addition of unsubstituted anthracene without a carboxylate group has no effect on the MLCT absorption band of  $[\text{Ru}(\text{bpy})_2(\text{biimH}_2)]^{2+}$  in dichloromethane.

The luminescence spectra of Figure 4a also provide evidence for cation–anion interactions. Upon addition of anthracene-9-carboxylate, both the luminescence intensity and band shape are changed. The alterations in the luminescence band shape are qualitatively similar to those observed in the absorption band (Figure 3a): There is a redshift of the  $^3\text{MLCT}$  emission band maximum between 0.00 and

1.25 equiv. of anthracene-9-carboxylate that amounts to roughly 35 nm. The apparent shape of the resulting luminescence spectra is that of a double band; however, the dip at 650 nm is merely an instrumental artifact. As in the absorption data, the redshift is essentially complete when 1.25 equiv. of anthracene-9-carboxylate is added, and further addition of this titrant only leads to decreasing luminescence intensities but does not affect the band shape any more.

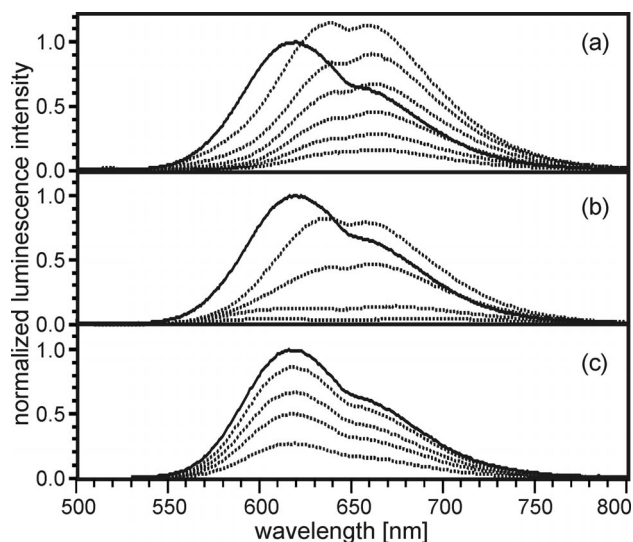


Figure 4.  $^3\text{MLCT}$  luminescence emitted by  $10^{-5}$  M  $\text{CH}_2\text{Cl}_2$  solutions of  $[\text{Ru}(\text{bpy})_2(\text{biimH}_2)]^{2+}$  in the presence of varying concentrations of three different titrants: (a) anthracene-9-carboxylate; (b) tetrabutylammonium hydroxide; (c) unsubstituted anthracene. Solid lines: spectra of pure  $[\text{Ru}(\text{bpy})_2(\text{biimH}_2)]^{2+}$  solutions without added titrant. Dotted lines: Spectra with decreasing intensity were obtained after addition of increasing amounts of titrants, specifically 0.42, 0.83, 1.25, 2.50, 5.00, and 10.00 equiv. for (a); 0.42, 1.25, 2.50, and 10.00 equiv. for (b); 3, 16, 90, and 280 equiv. for (c). Selective excitation of the metal complex occurred at the isosbestic point at 482 nm in all cases.

When  $[\text{Ru}(\text{bpy})_2(\text{biimH}_2)]^{2+}$  is deprotonated by the strong base tetrabutylammonium hydroxide, a redshift is also observed (Figure 4b). This behavior is in agreement with that observed above in  $^1\text{H}$  NMR and optical absorption spectroscopy, where there are close analogies between the effects of hydrogen-bond formation (with carboxylate) and deprotonation (with hydroxide). Associated with the addition of hydroxide is also a decrease in the emission intensity. Figure 4c shows that addition of unsubstituted anthracene to a dichloromethane solution of  $[\text{Ru}(\text{bpy})_2(\text{biimH}_2)]^{2+}$  also leads to emission quenching, but the band shape remains unaffected because of the absence of hydrogen-bond formation or deprotonation in this situation. Moreover, significantly larger quantities of unsubstituted anthracene are necessary to induce the same amount of quenching as with anthracene-9-carboxylate.

For the luminescence spectroscopic studies (Figures 4 and 5), the ruthenium complexes were excited at 482 nm, a wavelength corresponding to an isosbestic point in the optical absorption spectra in Figure 3. Figure 5 shows the re-

sults of a luminescence intensity titration of  $[\text{Ru}(\text{bpy})_2(\text{biimH}_2)]^{2+}$  in dichloromethane with the three different titrants from above. Initial addition of anthracene-9-carboxylate (circles) and tetrabutylammonium hydroxide (triangles) leads to an increase in the emission intensity by 35 and 45 percent, respectively. The maximum luminescence intensities are reached when approximately 0.2 equiv. of carboxylate/hydroxide titrants are added, and subsequently the emission intensity decreases steeply in both cases.

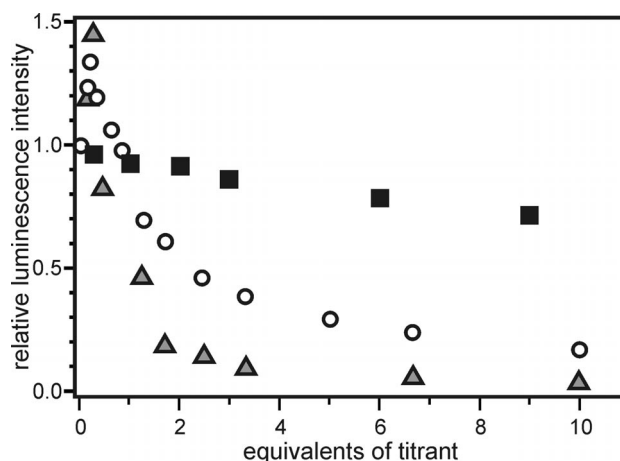


Figure 5. Normalized luminescence intensity as a function of number of equivalents of titrant added to a  $10^{-5}$  M  $\text{CH}_2\text{Cl}_2$  solution of  $[\text{Ru}(\text{bpy})_2(\text{biimH}_2)]^{2+}$ . Open circles: anthracene-9-carboxylate; gray filled triangles: tetrabutylammonium hydroxide; black filled squares: unsubstituted anthracene. Excitation of the metal complex occurred at the isosbestic point at 482 nm in all cases. The luminescence intensity of the initial solution containing pure  $[\text{Ru}(\text{bpy})_2(\text{biimH}_2)]^{2+}$  was set to a value of 1.0.

A prior study on the  $[\text{Ru}(\text{bpy})_2(\text{biimH}_2)]^{2+}$  complex already showed that the mono-deprotonated congener,  $[\text{Ru}(\text{bpy})_2(\text{biimH})]^+$ , has a drastically reduced emission quantum yield relative to that of the parent complex.<sup>[11a]</sup> The decrease in the emission intensity upon addition of the strong hydroxide base (triangles) therefore comes as no surprise. More intriguing is the initial increase in the emission intensities observed for both anthracene-9-carboxylate and hydroxide. In the  $[\text{Ru}(\text{bpy})_2(\text{biimH}_2)]^{2+}$  complex, luminescence is in competition with the deactivation of the MLCT excited state by nonradiative relaxation. The highest-frequency vibrations are usually the most effective for multiphonon relaxation;<sup>[14]</sup> hence, the biimidazole N–H vibrations and the interaction of these hydrogen atoms with the solvent are particularly important for nonradiative excited-state deactivation in the ruthenium complex considered here. Prior work on emissive biimidazole complexes in apolar solution has already shown that the addition of anions that participate in hydrogen bonding may lead to increased emission intensities.<sup>[8e,9a]</sup> Thus far, the origin of this effect may only be speculated, but given the above-mentioned special role of the N–H vibrations, it is not particularly surprising that hydrogen-bond formation affects the luminescence intensities of these biimidazole complexes. It has been argued that the N–H vibrational frequency is low-



ered upon N–H–O hydrogen-bond formation, thereby decreasing the efficiency of multiphonon relaxation.<sup>[8e]</sup> This may explain the initial increase in the emission intensity upon addition of anthracene-9-carboxylate (circles). As far as the data for hydroxide addition is concerned (triangles), the formation of hydrogen-bonded metal complex dimers may potentially be held responsible for the initial increase that is observed in the luminescence intensity titration. It is known that mono-deprotonated biimidazole complexes may form hydrogen-bonded dimers with fairly high association constants.<sup>[8e,15]</sup> In these dimers, one biimidazole ligand from each metal complex acts simultaneously as a hydrogen-bond donor at one nitrogen site and as a hydrogen-bond acceptor at the second noncoordinated nitrogen atom. The formation of these N–H–N hydrogen bonds can be expected to affect the N–H vibration energy in a similar way as do the above-mentioned N–H–O hydrogen bonds, and an analogous decrease in the efficiency of multiphonon relaxation may therefore result. Superimposed on this effect is the influence of the weakly emitting mono-deprotonated  $[\text{Ru}(\text{bpy})_2(\text{biimH})]^+$  complexes that are part of the hydrogen bond dimer equilibrium but not actually involved in hydrogen bonding to other complexes. Apparently, their influence on the emission intensity becomes dominant at values of added hydroxide that are greater than 0.2 equiv.

Figure 5 shows that addition of unsubstituted anthracene to a dichloromethane solution of  $[\text{Ru}(\text{bpy})_2(\text{biimH}_2)]^{2+}$  does also lead to a decrease of the luminescence intensity emitted by the ruthenium complex (squares), albeit to a lesser extent than the addition of anthracene-9-carboxylate, which can participate in hydrogen bonding (circles). Characteristic for anthracene is an energetically relatively low-lying triplet excited state at approximately 1.8 eV above the ground state.<sup>[16]</sup> Hence, this molecule is a popular choice as an energy acceptor in donor–acceptor systems that aim to explore photoinduced energy transfer with transition metal photosensitizers such as ruthenium polypyridyl compounds or rhenium tricarbonyl diimines.<sup>[17]</sup> The energetically lowest-lying <sup>3</sup>MLCT state of  $[\text{Ru}(\text{bpy})_2(\text{biimH}_2)]^{2+}$  is approximately 2.1 eV above the ground state; hence, energy transfer from this complex to anthracene is expected to be exergonic by roughly 0.3 eV. Prior work in the area of photoinduced electron transfer has demonstrated that hydrogen bonds can mediate relatively strong electronic coupling,<sup>[4]</sup> and one might thus expect triplet–triplet (Dexter-type) energy transfer to occur with particular ease in hydrogen-bonded 1:1 adducts between  $[\text{Ru}(\text{bpy})_2(\text{biimH}_2)]^{2+}$  and anthracene-9-carboxylate. The stronger luminescence quenching observed in Figure 5 for anthracene-9-carboxylate (circles) with respect to unsubstituted anthracene (squares) suggests that this is indeed the case.

Conclusive evidence for energy transfer in the  $[\text{Ru}(\text{bpy})_2(\text{biimH}_2)]^{2+}$ –anthracene-9-carboxylate system comes from the transient absorption data in Figure 6. The uppermost panel (a) shows transient absorption spectra of 1:1 mixtures of the ruthenium complex with anthracene-9-carboxylate (solid trace) and unsubstituted anthracene (dotted trace) at a concentration of  $10^{-5}$  M in dichloromethane. In the middle

panel (b) there are analogous data obtained from the same 1:1 mixtures but further diluted to  $10^{-6}$  M. The spectra in the uppermost panel are clearly identifiable as the spectroscopic signatures of the lowest anthracene triplet excited state, even though there are slight differences (ca. 2 nm) between the band maxima of anthracene-9-carboxylate and unsubstituted anthracene. When the  $10^{-5}$  M solutions are further diluted, the intensity of the transient absorption signal of unsubstituted anthracene decreases more strongly than that of anthracene-9-carboxylate, and at a dilution of  $10^{-6}$  M (Figure 6b), the signal due to unsubstituted anthracene is not observable any more. This suggests that, under these very dilute conditions, the remaining transient absorption signal is predominantly due to energy-transfer products that are part of a hydrogen-bonded donor–acceptor pair. This, in turn, would imply an association constant ( $K_a$ ) between  $[\text{Ru}(\text{bpy})_2(\text{biimH}_2)]^{2+}$  and anthracene-9-carboxylate that is of the order of  $10^5$ – $10^6$  M<sup>−1</sup>, a value that is in line with previously reported  $K_a$  values for comparable systems.<sup>[9a,10]</sup> We note that, at a 1:1 ratio of  $[\text{Ru}(\text{bpy})_2(\text{biimH}_2)]^{2+}$  and anthracene-9-carboxylate, the formation of donor–acceptor pairs as shown in Scheme 1a is consistent with the <sup>1</sup>H NMR spectroscopic data presented above. Finally, the bottom panel of Figure 6 shows the transient absorption spectrum measured in a  $3 \times 10^{-6}$  M dichloromethane solution of the covalent donor-bridge-acceptor molecule shown in Scheme 1b. Essentially the same triplet spectrum is observed as that for anthracene-9-carboxylate and free anthracene.

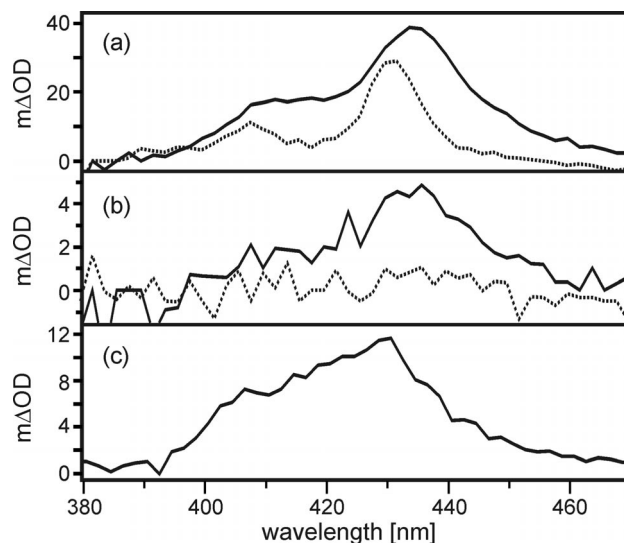


Figure 6. (a) Transient absorption spectra of 1:1 mixtures of  $[\text{Ru}(\text{bpy})_2(\text{biimH}_2)]^{2+}$  with anthracene-9-carboxylate (solid trace) and  $[\text{Ru}(\text{bpy})_2(\text{biimH}_2)]^{2+}$  with unsubstituted anthracene (dotted trace) in  $\text{CH}_2\text{Cl}_2$  at concentrations of  $10^{-5}$  M; (b) the same experiments at a dilution of  $10^{-6}$  M; (c) transient absorption spectrum of the donor-bridge-acceptor molecule shown in Scheme 1b in  $3 \times 10^{-6}$  M  $\text{CH}_2\text{Cl}_2$  solution. In all experiments, the excitation wavelength was 532 nm, and detection occurred in a 10  $\mu\text{s}$  time window starting 1  $\mu\text{s}$  after excitation with 10 ns laser pulses.

The upper half of Figure 7 shows the temporal evolution of the transient absorption signal from Figure 6b for the  $[\text{Ru}(\text{bpy})_2(\text{biimH}_2)]^{2+}$ –anthracene-9-carboxylate 1:1 adduct. The population of the anthracene-9-carboxylate triplet excited state builds up exponentially with a time constant of 153 ns (Figure 7a) and decays in a single-exponential manner with a time constant of 59  $\mu\text{s}$  (Figure 7b) in deoxygenated dichloromethane solution. Lifetimes of this order of magnitude are typical for aromatic triplet excited states.<sup>[16]</sup> More interesting is the build-up of the triplet anthracene population, from which one extracts a rate constant for energy transfer ( $k_{\text{EnT}}$ ) from the ruthenium complex to anthracene-9-carboxylate of  $6.5 \times 10^6 \text{ s}^{-1}$ . Figure 7c shows that, in the covalent donor-bridge-acceptor molecule shown in Scheme 1b, the triplet anthracene population as monitored at 430 nm builds up with a time constant of 10 ns. Indeed, this time constant is instrumentally limited, and we may only estimate a lower limit of  $10^8 \text{ s}^{-1}$  for the energy-transfer rate constant ( $k_{\text{EnT}}$ ) in this case. The anthracene triplet excited state in this molecule has a lifetime of 51  $\mu\text{s}$  (Figure 7d). However, the key point here is that  $k_{\text{EnT}}$  is at least 15 times larger for the covalent system than for the salt bridge adduct.

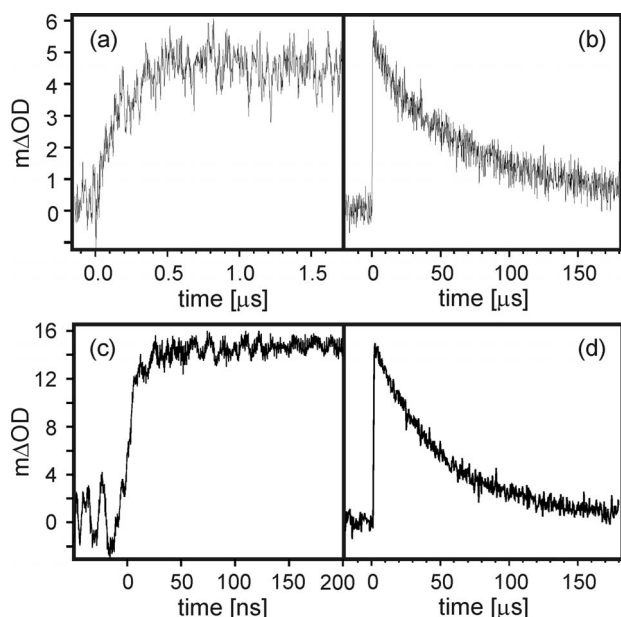


Figure 7. (a) Rise of the transient absorption signal in Figure 6b ( $10^{-6} \text{ M}$   $[\text{Ru}(\text{bpy})_2(\text{biimH}_2)]^{2+}$ –anthracene-9-carboxylate 1:1 mixture in  $\text{CH}_2\text{Cl}_2$ ) as detected at 436 nm; (b) decay of the same signal; (c) rise of the transient absorption signal in Figure 6c detected at 430 nm ( $3 \times 10^{-6} \text{ M}$  solution of the donor-bridge-acceptor molecule shown in Scheme 1b in  $\text{CH}_2\text{Cl}_2$ ); (d) decay of the same signal. Excitation occurred at 532 nm with laser pulses of 10 ns duration in all four cases. The solutions were deoxygenated by three subsequent freeze-pump-thaw cycles. Note the different time scales in panels (a) and (c).

By analogy to numerous other  $\text{d}^6$ -metal(diimine)–arene donor–acceptor systems,<sup>[17]</sup> triplet–triplet energy transfer in the systems shown in Scheme 1 is expected to occur by means of a through-bond electron exchange process. On the basis of X-ray crystal structures for related biimidazole

complexes that form hydrogen-bonded 1:1 cation–anion adducts with benzoates,<sup>[7c,9a]</sup> one arrives at an estimate of approximately 10 Å for the distance between the ruthenium(II) ion and the anthracene core in the hydrogen-bonded  $[\text{Ru}(\text{bpy})_2(\text{biimH}_2)]^{2+}$ –anthracene-9-carboxylate adduct shown in Scheme 1a. This compares to a ruthenium–anthracene distance of approximately 10.6 Å in the covalent donor-bridge-acceptor molecule shown in Scheme 1b. Thus, the donor–acceptor distances are nearly identical in the two cases investigated here. There are only minor differences in the driving forces for ruthenium-to-anthracene energy transfer between the two systems shown in Scheme 1, and hence the difference in  $k_{\text{EnT}}$  is likely a manifestation of differences in electronic couplings that are mediated by the salt bridge on the one hand and the covalent *p*-xylene spacer on the other hand. Dexter-type triplet–triplet energy-transfer rate constants ( $k_{\text{EnT}}$ ) are proportional to the squared matrix elements for overall electronic donor–acceptor coupling ( $H_{\text{DA}}$ ).<sup>[18]</sup> Therefore,  $H_{\text{DA}}$  must be larger at least by a factor of 4 for the xylene-bridged system than for the salt bridge adduct. Calculation of a more exact number is hampered by our inability to determine  $k_{\text{EnT}}$  values that are greater than  $10^8 \text{ s}^{-1}$ , but an upper limit for  $k_{\text{EnT}}$  of  $10^{10} \text{ s}^{-1}$  appears plausible in view of a recent study that reports on ruthenium-to-anthracene energy transfer across a flexible alkane spacer.<sup>[19]</sup> In this system, the donor–acceptor distance is roughly 8.5 Å, but since alkane spacers mediate charge and energy transfer less efficiently than  $\pi$ -conjugated spacers,<sup>[20]</sup> the above-mentioned upper limit of  $k_{\text{EnT}} = 10^{10} \text{ s}^{-1}$  seems reasonable for the somewhat longer *p*-xylene bridged system shown in Scheme 1b.<sup>[21]</sup> We thus arrive at an estimated upper limit of a factor of 40 for the difference in electronic donor–acceptor coupling ( $H_{\text{DA}}$ ) between the salt bridge and a covalent linker. This finding is in line with recent comparative studies of photoinduced electron tunneling through hydrogen-bonding and non-hydrogen-bonding solvent matrices that have provided evidence for comparatively strong electronic coupling across this type of intermolecular bond.<sup>[22]</sup> As has been pointed out recently, the weaker electronic coupling across salt bridge interfaces with respect to that across covalent bonds may not only be the result of smaller orbital overlaps, but it may also be influenced by differences in the HOMO and LUMO energies of the bridging units that separate the donor from the acceptor.<sup>[23]</sup> Be that as it may, it is clear that triplet–triplet energy transfer across salt bridge interfaces, whether of guanidinium–carboxylate<sup>[23–24]</sup> or biimidazole–carboxylate type,<sup>[10]</sup> is relatively efficient even when compared to covalent bonds.

## Conclusions

The spectroscopic evidence presented in this paper indicates that, in dichloromethane solution, more than one anthracene-9-carboxylate anion can interact closely with the dicationic  $[\text{Ru}(\text{bpy})_2(\text{biimH}_2)]^{2+}$  complex. This is in spite of the presence of only one single biimidazole ligand that is

available for formation of doubly hydrogen-bonded cation–anion pairs in a salt bridge. Energy transfer across this salt bridge in highly diluted 1:1 cation–anion adducts is substantially more efficient than energy transfer between  $[\text{Ru}(\text{bpy})_2(\text{biimH}_2)]^{2+}$  and unsubstituted anthracene, but slower at least by a factor of 15 than the intramolecular energy transfer over roughly the same distance from a  $[\text{Ru}(\text{bpy})_3]^{2+}$  unit to a covalently attached anthracene acceptor. Yet, electronic donor–acceptor coupling in the supramolecular adduct is estimated to be smaller than that in the covalent system only by a factor of 4 to 40. Salt bridges seem therefore well suited for the construction of complicated supramolecular structures in which efficient energy or charge transfer is desired.

## Experimental Section

$[\text{Ru}(\text{bpy})_2(\text{biimH}_2)]^{2+}$  was synthesized as a hexafluorophosphate salt as described previously, and characterization data are as reported in two prior studies.<sup>[12b,25]</sup> Anthracene-9-carboxylic acid was bought from the Sigma–Aldrich chemical company and converted to anthracene-9-carboxylate by use of tetrabutylammonium hydroxide. The latter, as well as unsubstituted anthracene, was also bought from Sigma–Aldrich.

The covalent donor-bridge-acceptor molecule shown in Scheme 1b was synthesized by following the same synthetic strategy that we used in our prior work on donor-bridge-acceptor systems for intramolecular electron transfer.<sup>[26]</sup> Detailed synthetic protocols and product characterization data are presented in the Supporting Information

Dichloromethane of spectrophotometric grade was used for the optical spectroscopic experiments.  $^1\text{H}$  NMR spectroscopy, UV/Vis optical absorption, emission, and transient absorption experiments were performed with the instruments described in some of our prior publications.<sup>[26]</sup>

**Supporting Information** (see footnote on the first page of this article): Synthetic protocols and product characterization data for the synthesis of the covalent donor-bridge-acceptor molecule shown in Scheme 1b.

## Acknowledgments

Financial support by the Swiss National Science Foundation through grant number PP002-110611 is acknowledged. The University of Geneva is thanked for hosting our group while much of the research presented herein was performed.

- [1] a) P. D. Beer, P. A. Gale, *Angew. Chem. Int. Ed.* **2001**, *40*, 486–516; b) V. Amendola, L. Fabbrizzi, *Chem. Commun.* **2009**, 513–531; c) K. M. Mullen, P. D. Beer, *Chem. Soc. Rev.* **2009**, *38*, 1701–1713; d) V. Amendola, D. Esteban-Gómez, L. Fabbrizzi, M. Licchelli, *Acc. Chem. Res.* **2006**, *39*, 343–353.
- [2] a) K. T. Holman, A. M. Pivovar, J. A. Swift, M. D. Ward, *Acc. Chem. Res.* **2001**, *34*, 107–118; b) Y. Nakatani, Y. Furusho, E. Yashima, *Angew. Chem. Int. Ed.* **2010**, *49*, 5463–5467; c) M. Tadokoro, S. Fukui, T. Kitajima, Y. Nagao, S. Ishimaru, H. Kitagawa, K. Isobe, K. Nakasuji, *Chem. Commun.* **2006**, 1274–1276.
- [3] a) B. Musafia, V. Buchner, D. Arad, *J. Mol. Biol.* **1995**, *254*, 761–770; b) P. Strop, S. L. Mayo, *Biochemistry* **2000**, *39*, 1251–1255.
- [4] J. C. Chang, J. D. K. Brown, M. C. Y. Chang, E. A. Baker, D. G. Nocera in *Electron Transfer in Chemistry*, Vol. 3 (Ed.: V. Balzani), VCH Wiley, Weinheim, **2001**, pp. 409–461.
- [5] a) A. Dirksen, C. J. Kleverlaan, J. N. H. Reek, L. De Cola, *J. Phys. Chem. A* **2005**, *109*, 5248–5256; b) M. D. Ward, C. M. White, F. Barigelletti, N. Armaroli, G. Calogero, L. Flamigni, *Coord. Chem. Rev.* **1998**, *171*, 481–488; c) J. L. Sessler, M. Sathiosatham, C. T. Brown, T. A. Rhodes, G. Wiederrecht, *J. Am. Chem. Soc.* **2001**, *123*, 3655–3660; d) T. Torres, A. Gouloumis, D. Sanchez-Garcia, J. Jayawickramarajah, W. Seitz, D. M. Guldi, J. L. Sessler, *Chem. Commun.* **2007**, 292–294; e) G. Bergamini, C. Sautan, P. Ceroni, M. Maestri, V. Balzani, M. Gorka, S. K. Lee, J. van Heyst, F. Vögtle, *J. Am. Chem. Soc.* **2004**, *126*, 16466–16471; f) F. Loiseau, G. Marzanni, S. Quici, M. T. Indelli, S. Campagna, *Chem. Commun.* **2003**, 286–287; g) E. H. A. Beckers, P. A. van Hal, A. P. H. J. Schenning, A. El-ghayoury, E. Peeters, M. T. Rispen, J. C. Hummelen, E. W. Meijer, R. A. J. Janssen, *J. Mater. Chem.* **2002**, *12*, 2054–2060; h) M. D. Ward, *Chem. Soc. Rev.* **1997**, *26*, 365–375.
- [6] a) J. A. Roberts, J. P. Kirby, D. G. Nocera, *J. Am. Chem. Soc.* **1995**, *117*, 8051–8052; b) Y. Q. Deng, J. A. Roberts, S. M. Peng, C. K. Chang, D. G. Nocera, *Angew. Chem. Int. Ed. Engl.* **1997**, *36*, 2124–2127; c) N. H. Damrauer, J. M. Hodgkiss, J. Rosenthal, D. G. Nocera, *J. Phys. Chem. B* **2004**, *108*, 6315–6321; d) J. Rosenthal, J. M. Hodgkiss, E. R. Young, D. G. Nocera, *J. Am. Chem. Soc.* **2006**, *128*, 10474–10483.
- [7] a) S. Fortin, A. L. Beauchamp, *Inorg. Chem.* **2001**, *40*, 105–112; b) B. B. Ding, Y. Q. Weng, Z. W. Mao, C. K. Lam, X. M. Chen, B. H. Ye, *Inorg. Chem.* **2005**, *44*, 8836–8845; c) S. Rau, L. Böttcher, S. Schebesta, M. Stollenz, H. Görls, D. Walther, *Eur. J. Inorg. Chem.* **2002**, 2800–2809; d) A. Grüssing, S. Rau, S. Schebesta, A. Scholz, H. Görls, D. Walther, *Z. Anorg. Allg. Chem.* **2007**, *633*, 961–970; e) R. L. Sang, X. Li, *Inorg. Chim. Acta* **2006**, *359*, 525–532.
- [8] a) S. Fortin, P. L. Fabre, M. Dartiguenave, A. L. Beauchamp, *J. Chem. Soc., Dalton Trans.* **2001**, 3520–3527; b) Y. Cui, H. J. Mo, J. C. Chen, Y. L. Niu, Y. R. Zhong, K. C. Zheng, B. H. Ye, *Inorg. Chem.* **2007**, *46*, 6427–6436; c) A. Maiboroda, G. Rheinwald, H. Lang, *Eur. J. Inorg. Chem.* **2001**, 2263–2269; d) R. Atencio, K. Ramírez, J. A. Reyes, T. González, P. Silva, *Inorg. Chim. Acta* **2005**, *358*, 520–526; e) S. Derossi, H. Adams, M. D. Ward, *Dalton Trans.* **2007**, 33–36; f) J. Perez, L. Riera, *Chem. Commun.* **2008**, 533–543.
- [9] a) J. C. Freys, G. Bernardinelli, O. S. Wenger, *Chem. Commun.* **2008**, 4267–4269; b) J. C. Freys, D. Hanss, M. E. Walther, O. S. Wenger, *Chimia* **2009**, *63*, 49–53.
- [10] S. Rau, B. Schäfer, S. Schebesta, A. Grüssing, W. Poppitz, D. Walther, M. Duati, W. R. Browne, J. G. Vos, *Eur. J. Inorg. Chem.* **2003**, 1503–1506.
- [11] a) M. Haga, *Inorg. Chim. Acta* **1983**, *75*, 29–35; b) E. V. Dose, L. J. Wilson, *Inorg. Chem.* **1978**, *17*, 2660–2666.
- [12] a) B. P. Sullivan, D. J. Salmon, T. J. Meyer, J. Peedin, *Inorg. Chem.* **1979**, *18*, 3369–3374; b) A. M. Bond, M. Haga, *Inorg. Chem.* **1986**, *25*, 4507–4514; c) M. Haga, T. Ano, K. Kano, S. Yamabe, *Inorg. Chem.* **1991**, *30*, 3843–3849; d) R. F. Carina, L. Verzeqnessi, G. Bernardinelli, A. F. Williams, *Chem. Commun.* **1998**, 2681–2682; e) M. Leirer, G. Knör, A. Vogler, *Inorg. Chim. Acta* **1999**, *288*, 150–153; f) H. Jones, M. Newell, C. Metcalfe, S. E. Spey, H. Adams, J. A. Thomas, *Inorg. Chem. Commun.* **2001**, *4*, 475–477; g) G. Stupka, L. Gremaud, G. Bernardinelli, A. F. Williams, *Dalton Trans.* **2004**, 407–412.
- [13] K. M. Lancaster, J. B. Gerken, A. C. Durrell, J. H. Palmer, H. B. Gray, *Coord. Chem. Rev.* **2010**, *254*, 1803–1811.
- [14] T. C. Brunold, H. U. Güdel in *Inorganic Electronic Structure and Spectroscopy*, Vol. 1 (Eds.: E. I. Solomon, A. B. P. Lever), Wiley, New York, **1999**, pp. 259–306.
- [15] a) M. Tadokoro, J. Toyoda, K. Isobe, T. Itoh, A. Miyazaki, T. Enoki, K. Nakasuji, *Chem. Lett.* **1995**, 613–614; b) M. Tadokoro, H. Kanno, T. Kitajima, H. Shimada-Umemoto, N. Nak-



- anishi, K. Isobe, K. Nakasuji, *Proc. Natl. Acad. Sci. USA* **2002**, *99*, 4950–4955.
- [16] N. J. Turro, *Molecular Photochemistry*, New York, Amsterdam, **1967**.
- [17] a) S. Boyde, G. F. Strouse, W. E. Jones, T. J. Meyer, *J. Am. Chem. Soc.* **1989**, *111*, 7448–7454; b) J. A. Simon, S. L. Curry, R. H. Schmehl, T. R. Schatz, P. Piotrowiak, X. Q. Jin, R. P. Thummel, *J. Am. Chem. Soc.* **1997**, *119*, 11012–11022; c) B. Maubert, N. D. McClenaghan, M. T. Indelli, S. Campagna, *J. Phys. Chem. A* **2003**, *107*, 447–455; d) G. J. Wilson, A. Launikonis, W. H. F. Sasse, A. W. H. Mau, *J. Phys. Chem. A* **1997**, *101*, 4860–4866; e) Z. Murtaza, D. K. Graff, A. P. Zipp, L. A. Worl, W. E. Jones, W. D. Bates, T. J. Meyer, *J. Phys. Chem.* **1994**, *98*, 10504–10513; f) K. S. Schanze, D. B. MacQueen, T. A. Perkins, L. A. Cabana, *Coord. Chem. Rev.* **1993**, *122*, 63–89; g) M. E. Walther, O. S. Wenger, *Dalton Trans.* **2008**, 6311–6318.
- [18] C. P. Hsu, *Acc. Chem. Res.* **2009**, *42*, 509–518.
- [19] J. R. Schoonover, D. M. Dattelbaum, A. Malko, V. I. Klimov, T. J. Meyer, D. J. Styers-Barnett, E. Z. Gannon, J. C. Granger, W. S. Aldridge, J. M. Papanikolas, *J. Phys. Chem. A* **2005**, *109*, 2472–2475.
- [20] H. B. Gray, J. R. Winkler, *Proc. Natl. Acad. Sci. USA* **2005**, *102*, 3534–3539.
- [21] We also note that in our covalent dyad the *p*-xylene–anthracene moiety is attached to the 5-position at the bipyridine ligand, which is known to provide weaker electronic coupling (and hence slower electron transfer) than substitution at the 4-position. We used 5-bromo-2,2'-bipyridine as a precursor, because its synthesis is more straightforward than that of 4-bromo-2,2'-bipyridine.
- [22] a) A. Ponce, H. B. Gray, J. R. Winkler, *J. Am. Chem. Soc.* **2000**, *122*, 8187–8191; b) O. S. Wenger, B. S. Leigh, R. M. Villahermosa, H. B. Gray, J. R. Winkler, *Science* **2005**, *307*, 99–102; c) O. S. Wenger, *Coord. Chem. Rev.* **2009**, *253*, 1439–1457; d) O. S. Wenger, *Acc. Chem. Res.* **2010**, DOI: 10.1021/ar100092v.
- [23] J. Otsuki, Y. Kanazawa, A. Kaito, D. M. S. Islam, Y. Araki, O. Ito, *Chem. Eur. J.* **2008**, *14*, 3776–3784.
- [24] L. Han, H. X. Wei, S. Y. Li, J. P. Chen, Y. Zeng, Y. Y. Li, Y. B. Han, Y. Li, S. Q. Wang, G. Q. Yang, *ChemPhysChem* **2010**, *11*, 229–235.
- [25] D. P. Rillema, R. Sahai, P. Matthews, A. K. Edwards, R. J. Shaver, L. Morgan, *Inorg. Chem.* **1990**, *29*, 167–175.
- [26] a) D. Hanss, O. S. Wenger, *Inorg. Chem.* **2009**, *48*, 671–680; b) D. Hanss, O. S. Wenger, *Eur. J. Inorg. Chem.* **2009**, 3778–3790; c) D. Hanss, J. C. Freys, G. Bernardinelli, O. S. Wenger, *Eur. J. Inorg. Chem.* **2009**, 4850–4859; d) M. E. Walther, O. S. Wenger, *ChemPhysChem* **2009**, *10*, 1203–1206; e) D. Hanss, O. S. Wenger, *Inorg. Chem.* **2008**, *47*, 9081–9084; f) D. Hanss, M. E. Walther, O. S. Wenger, *Chem. Commun.* **2010**, *46*, 7034–7036; g) M. E. Walther, J. Grilj, D. Hanss, E. Vauthey, O. S. Wenger, *Eur. J. Inorg. Chem.* **2010**, 4843–4850; h) D. Hanss, M. E. Walther, O. S. Wenger, *Coord. Chem. Rev.* **2010**, *254*, 2584–2592.

Received: July 28, 2010

Published Online: November 4, 2010